

Quadrupole moments and g factors for high-spin neutron isomers in ^{193}Pb

M. Ionescu-Bujor,¹ A. Iordachescu,¹ D. L. Balabanski,^{2,3} S. Chmel,⁴ G. Neyens,² G. Baldsiefen,⁴ D. Bazzacco,⁵ F. Brandolini,⁵ D. Bucurescu,¹ M. Danchev,³ M. De Poli,⁶ G. Georgiev,⁷ A. G6rgen,⁴ H. Haas,⁸ H. H6bel,⁴ G. Ilie,^{1,9} N. Marginean,^{1,6} R. Menegazzo,⁵ P. Pavan,⁵ G. Rainovski,^{3,10} R. V. Ribas,¹¹ C. Rossi Alvarez,⁵ C. A. Ur,^{1,5} K. Vyvey,² and S. Frauendorf^{12,13}

¹National Institute for Physics and Nuclear Engineering, Bucharest, Romania

²IKS, Katholieke Universiteit Leuven, Celestijnenlaan 200 D, B-3001 Leuven, Belgium

³Faculty of Physics, St. Kliment Ohridski University of Sofia, BG-1164 Sofia, Bulgaria

⁴Helmholtz-Institute f6ur Strahlen- und Kernphysik, Universit6at Bonn, Germany

⁵Dipartimento di Fisica dell' Universit6a and INFN, Sezione di Padova, Padova, Italy

⁶INFN, Laboratori Nazionali di Legnaro, Legnaro, Italy

⁷Grand Acc6el6rateur National d'Ions Lourds, F-14076 Caen Cedex 5, France

⁸Hahn-Meitner Institut, Bereich Festkorperphysik, D-14109 Berlin, Germany

⁹Faculty of Physics, University of Bucharest, Romania

¹⁰Department of Physics, University of Liverpool, Liverpool L69 7ZE, United Kingdom

¹¹Instituto de Fisica, Universidade de S6o Paulo, S6o Paulo, Brasil

¹²Institut f6ur Kern- und Hadronenphysik, Forschungszentrum Rossendorf, D-01314 Dresden, Germany

¹³Department of Physics, University of Notre Dame, Notre Dame, Indiana 46556, USA

(Received 20 May 2004; published 15 September 2004)

The g factors and quadrupole moments of the $21/2^-$ and $33/2^+$ isomers in ^{193}Pb have been measured by the time-differential perturbed γ -ray angular distribution method as $g(21/2^-) = -0.059(11)$, $|Q(21/2^-)| = 0.22(2)$ eb and $g(33/2^+) = -0.171(9)$, $|Q(33/2^+)| = 0.45(4)$ eb. The results support the three-neutron configurations $(1i_{13/2})^2_{12^+} \otimes 3p_{3/2}$ and $(1i_{13/2})^3$ for the $21/2^-$ and $33/2^+$ states, respectively. The quadrupole moment of the 12^+ isomer in ^{194}Pb described by the two-neutron $(1i_{13/2})^2$ configuration has been remeasured as $|Q(12^+)| = 0.48(3)$ eb in perfect agreement with the previous data. The experimental results are discussed within a microscopic Bardeen-Cooper-Schrieffer approach in a number-projected one- and three-quasiparticle neutron space, and in the frame of the pairing plus quadrupole tilted-axis cranking model.

DOI: 10.1103/PhysRevC.70.034305

PACS number(s): 21.10.Ky, 21.60.Cs, 21.60.Ev, 27.80.+w

I. INTRODUCTION

A large number of experimental and theoretical works has been devoted to the study of the neutron-deficient lead nuclei, as their structure exhibits a variety of interesting phenomena. Rather complex level schemes, involving in many cases isomeric states, have been established via in-beam and decay studies [1–4]. The spherical structures observed in these nuclei are associated with the proton shell closure at $Z=82$, and have been interpreted in various phenomenological and microscopical approaches involving neutron quasiparticle excitations [5–8]. These spherical neutron states are coexisting at low energies with more deformed states, associated with proton intruder particle-hole excitations across the closed shell [9]. In the even-mass isotopes, oblate deformed excitations of two-proton-two-hole structure occur as low-lying $I^\pi=0^+_2$ states as well as $I^\pi=8^+$ and $I^\pi=11^-$ high- K isomers [2]. In the odd-mass nuclei low-lying proton-based intruder states involving the coupling of the $1i_{13/2}$ or $3p_{3/2}$ odd quasineutron to the $I^\pi=0^+_2$ oblate state have been identified [3]. At high spin many sequences of magnetic dipole transitions with a rotational-like pattern have been found in the lead isotopes with $A=191$ – 202 [10,11]. These structures, known as magnetic-rotational bands [12], were interpreted as arising from the coupling of high- K two proton excitations into the $1h_{9/2}$ and $1i_{13/2}$ orbitals with neutron-hole

excitations in the $1i_{13/2}$ orbital. The description of these dipole bands has been extensively performed using the tilted axis cranking (TAC) model [13].

The knowledge of the static magnetic dipole and electric quadrupole moments is very important for elucidating the structure of coexisting states, as they are providing independent information on the underlying configurations and shapes, respectively. In the light lead nuclei with $A \leq 200$, g factors were measured for many low- and high-spin isomeric states [1] allowing configuration assignments. On the other hand the information on spectroscopic quadrupole moments in these nuclei is more limited. Such moments were reported for the $13/2^+$ and 12^+ states, involving one and two quasineutrons in the $1i_{13/2}$ orbital, in the odd-mass $^{191-197}\text{Pb}$ [14], and the even-mass $^{194-200}\text{Pb}$ [15–17], respectively, and rather small values, $|Q| \leq 0.8$ eb, were found, pointing to almost spherical shapes. In recent studies [18,19] the quadrupole moments of the 11^- isomers in $^{194,196}\text{Pb}$, described by the proton $(1h_{9/2}1i_{13/2})$ configuration, have been measured and much higher values [e. g. $|Q(11^-; ^{196}\text{Pb})| = 3.41(66)$ eb] have been reported, indicating a larger deformation associated with the intruder excitation. Up to now, no spectroscopic quadrupole moment was reported for states involving more than two quasiparticles in light lead nuclei.

Recently, an experimental study was undertaken at the XTU Tandem of the Laboratori Nazionali di Legnaro in or-

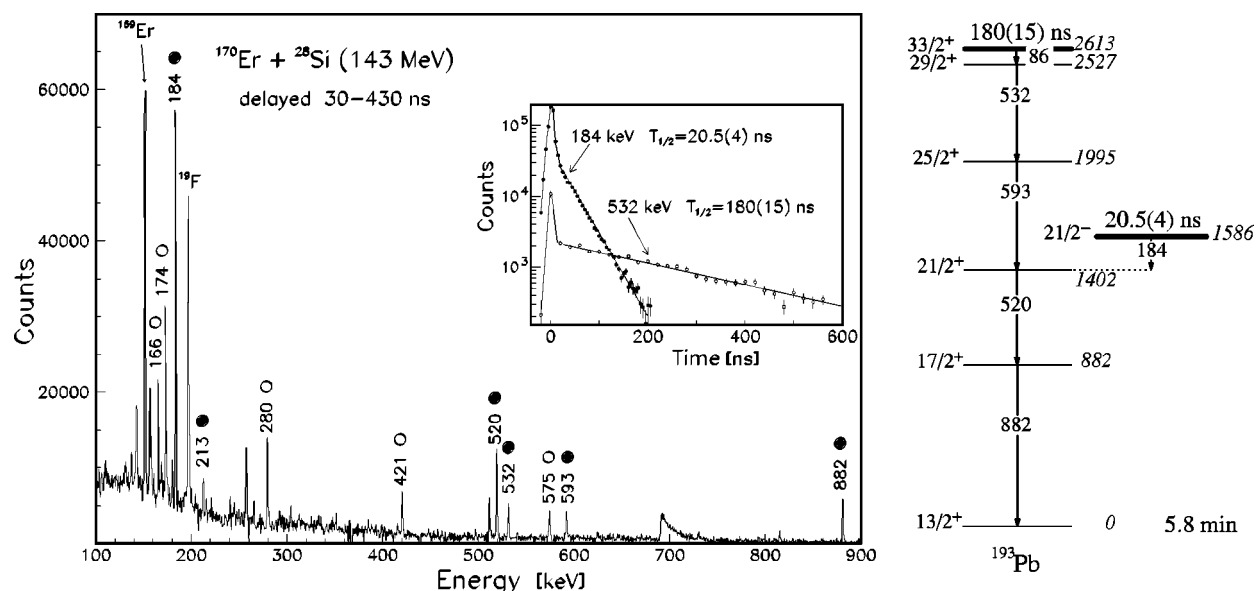


FIG. 1. Delayed γ spectrum corrected for the background due to long-lived activities (left) and partial level scheme of ^{193}Pb showing the decay of the $21/2^-$ and $33/2^+$ isomers [20] (right). The transitions assigned to ^{193}Pb and ^{194}Pb are labeled by energies and marked by full and open circles, respectively. In the inset are shown background corrected time spectra for delayed transitions. The excitation energies in the decay scheme are relative to the energy of the $13/2^+$ long-lived isomer.

der to determine the static electromagnetic moments for the high-spin short-lived isomeric states in ^{193}Pb . One objective of the study was to bring more insight into the underlying structure of the 9.4 ns $29/2^-$ isomeric state, bandhead of a magnetic-rotational band [20–22]. The results concerning the moments of this state are reported elsewhere [23,24]. The present paper is devoted to the investigation of the electromagnetic moments for two other short-lived isomers with spin-parities $21/2^-$ and $33/2^+$, known in ^{193}Pb [20]. The experimental details are presented in Sec. II. The experimental results are reported in Sec. III and discussed in the framework of the number-projected BCS and the pairing plus quadrupole approaches in Sec. IV. Conclusions are given in Sec. V. A part of the experimental data has been briefly reported in Ref. [25].

II. EXPERIMENTAL DETAILS

The isomeric states in ^{193}Pb were populated and aligned in the $^{170}\text{Er}(^{28}\text{Si}, 5n)$ reaction using a ^{28}Si pulsed beam of 143 MeV delivered by the XTU Tandem of the Laboratori Nazionali di Legnaro. The beam had a pulse of about 1.5 ns full width at half maximum (FWHM) and a repetition period of 400 ns in the g -factor experiment and of 800 ns in the quadrupole moment measurement. The method of time-differential observation of the perturbed angular distribution (TDPAD) of deexciting γ rays has been applied. The excited ^{193}Pb nuclei recoiled out of the thin Er target enriched in ^{170}Er to 97%, into the appropriately chosen hosts.

In the g -factor measurement the target consisted of 0.8 mg/cm^2 ^{170}Er foil rolled onto a 27 mg/cm^2 ^{208}Pb backing in which both the recoiling lead nuclei and the projectiles were stopped. The cubic structure of the lead crystalline lattice allowed the preservation of the nuclear alignment of the

excited ^{193}Pb nuclei. The target was placed between the pole tips of an electromagnet. A magnetic field $B=31.5(4)$ kG was applied perpendicular to the beam-detector plane and was periodically switched in direction. The γ rays were detected by two planar HPGe detectors and two HPGe detectors of 20% efficiency placed at $\pm 135^\circ$ and at $\pm 45^\circ$ to the beam direction, respectively.

The quadrupole interaction has been investigated in the electric field gradient (EFG) of the polycrystalline lattice of metallic solid Hg. The excited lead nuclei recoiled out of the 0.5 mg/cm^2 ^{170}Er foil into a solid 0.2 mm Hg layer mounted on a Cu cold finger held at the temperature $T=170.0(1)\text{K}$. The γ rays were detected by the planar HPGe detectors placed at 0° and 90° to the beam direction.

The time resolution for the planar detectors was about 10 and 6.5 ns at energies of 200 and 550 keV, respectively. For the detectors of 20% efficiency the time resolution at 550 keV was about 9 ns. These time resolutions were much smaller than the Larmor periods in the g -factor measurement (see Sec. III A) and the widths of the observed structures in the quadrupole moment measurement (see Sec. III B) and did not affect the analysis.

III. DATA ANALYSIS AND RESULTS

In the off-line analysis of list-mode data, two-dimensional matrices of energy versus time were formed for each detector. From these matrices time-gated energy spectra and energy-gated time spectra were created. A delayed γ spectrum obtained in the quadrupole interaction experiment, corresponding to the time interval of 30–430 ns after the beam burst, is illustrated in Fig. 1. The partial level scheme of ^{193}Pb showing the decay of the presently investigated isomers is shown in the right side of Fig. 1. For the $21/2^-$ state

the 184 keV isomeric transition was analyzed, while in the case of the $33/2^+$ isomer the analysis was done for the 532 and 593 keV transitions. The time spectra have been least squares fitted assuming an exponential decay. A constant background due to possible long-lived contaminants has been also allowed in fitting the data. This background was found to be almost zero. The decay curves for the 184 and 532 keV transitions, registered with the planar detectors, are shown as insets in Fig. 1. A half-life of $T_{1/2}=20.5(4)$ ns has been derived for the $21/2^-$ isomer, in agreement with the previous value of 22(2) ns [20]. The prompt component in the time spectrum of the 184 keV isomeric transition is due to the Coulomb excitation of $^{166,168}\text{Er}$, which appear as contaminations in the isotopically enriched ^{170}Er target. For the $33/2^+$ isomer the half-life $T_{1/2}=180(15)$ ns was determined, somewhat different from the previously determined value of $135^{(+25)}_{-15}$ ns [20].

After proper normalization, the time spectra $N(t, \theta)$ were used to construct the appropriate experimental ratios R_{exp} . They were least squares fitted to the theoretical expressions R_{theo} corresponding to the magnetic or quadrupole interaction (see below).

A. g factors

In the g -factor measurement the time spectra obtained for each of the two magnetic-field orientations were used to form the experimental modulation ratio

$$R_{\text{exp}}(t) = \frac{N_{\uparrow}(t) - N_{\downarrow}(t)}{N_{\uparrow}(t) + N_{\downarrow}(t)}, \quad (1)$$

which was least squares fitted to the expression

$$R_{\text{theo}}(t) = \frac{3}{4} A_2 \cos 2(\phi - \omega_L t), \quad (2)$$

with the angular distribution coefficient A_2 , the Larmor frequency $\omega_L = gB\mu_n/\hbar$, and the phase ϕ depending on the detector angle and the beam bending in the magnetic field as free parameters.

The modulation functions obtained from the time spectra of the 184 keV transition registered with the planar HPGe detectors are shown in Fig. 2. Due to the small interaction strength only a half-period of the Larmor oscillation could be observed. It shows an opposite phase in the two detectors placed at the angles $+135^\circ$ and -135° . From the least-squares analysis of these modulation curves, similar values within errors were obtained for the amplitude and Larmor frequency. The g factor which results from these data is $g(21/2^-) = -0.059(11)$.

For the $33/2^+$ isomer the time spectra for the 532 and 593 keV γ rays, registered with the large-volume HPGe detectors, were analyzed. The modulation ratio corresponding to the total accumulated statistics is illustrated in Fig. 3. The deduced g factor is $g(33/2^+) = -0.171(9)$.

The diamagnetic and Knight shift corrections were not applied. They are both small (about 1%) and opposite in sign [26], so they nearly cancel each other.

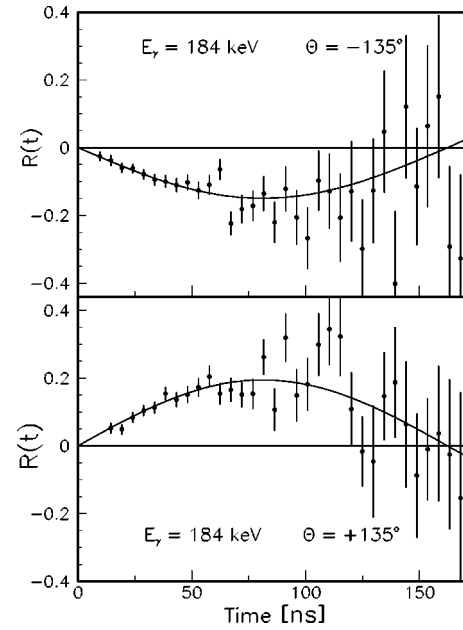


FIG. 2. Modulation ratios for the 184 keV γ ray deexciting the $21/2^-$ isomer in ^{193}Pb in an external magnetic field of 31.5 kG and the corresponding least-squares fits.

B. Quadrupole moments

In the case of an electric quadrupole interaction, the superposition of many frequency components leads to modulation spectra which can have quite a complicated structure depending on the nuclear spin I , the symmetry of the interaction, and the geometrical arrangement of the detectors. For an axially symmetric EFG the modulation spectra are periodic with the basic repetition quadrupole period T_o given by $T_o = 2I(2I-1)/3\nu_Q$ for a half-integer spin and by $T_o = 4I(2I-1)/3\nu_Q$ for an integer spin, where $\nu_Q = QV_{zz}/h$ is the quadrupole coupling constant depending on the spectroscopic quadrupole moment Q and the EFG strength V_{zz} .

The experimental ratio defined as

$$R_{\text{exp}}(t) = \frac{N(t, 0^\circ) - N(t, 90^\circ)}{N(t, 0^\circ) + N(t, 90^\circ)}, \quad (3)$$

was least squares fitted to the expression

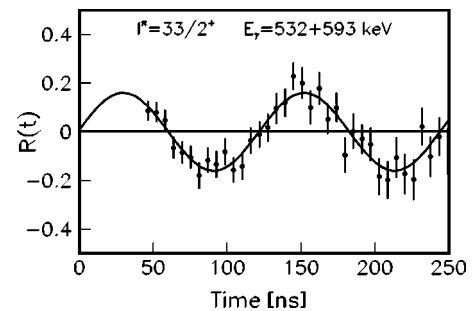


FIG. 3. Modulation ratio for the γ rays deexciting the $33/2^+$ isomer in ^{193}Pb in an external magnetic field of 31.5 kG and the least-squares fit.

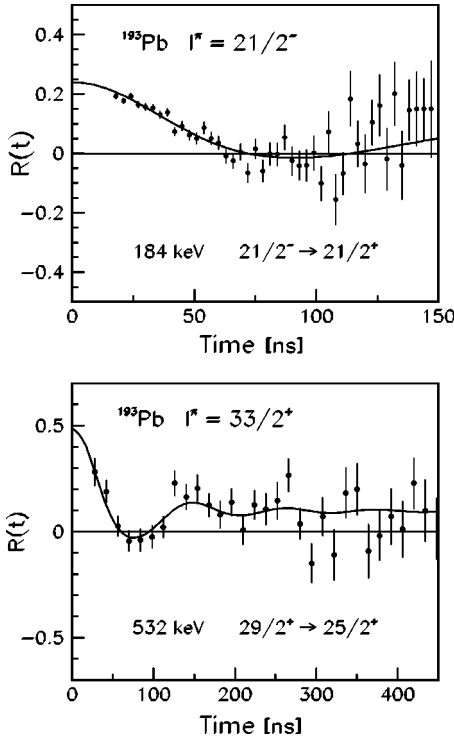


FIG. 4. Experimental and theoretical TDPAD spectra showing the quadrupole interaction of the $21/2^-$ and $33/2^+$ isomeric states of ^{193}Pb in solid Hg at a temperature of 170 K.

$$R_{\text{theo}}(t) = \frac{3}{4} A_2 \sum s_{2n} \cos(n\omega_0 t), \quad (4)$$

with the angular distribution coefficient A_2 and the quadrupole interaction frequency $\omega_0 = 2\pi/T_0$ as free parameters. The spin-dependent s_{2n} coefficients in the theoretical expression (4) are tabulated in Ref. [27] for an axially symmetric randomly oriented EFG.

Examples of the obtained quadrupole interaction pattern for the 184 and 532 keV γ transitions are shown in Fig. 4. Due to the high spin and short lifetime of the isomers, it was not possible to evidence the full quadrupole period T_0 and only the structure at the beginning of the modulation pattern could be observed. The deduced values for the quadrupole coupling constant were 91(7) and 191(14) MHz for the $21/2^-$ and $33/2^+$ states, respectively. With the EFG calibration of $V_{zz}(\text{PbHg}) = 17.4(9) \times 10^{21} \text{ V/m}^2$ at $T = 170 \text{ K}$, obtained by using data from Ref. [15], absolute values of spectroscopic quadrupole moments for the high-spin isomers in ^{193}Pb have been derived as $|Q(21/2^-)| = 0.22(2) \text{ eb}$ and $|Q(33/2^+)| = 0.45(4) \text{ eb}$.

In the present experiment, besides ^{193}Pb , the ^{194}Pb nucleus was also populated, through the $^{170}\text{Er}(^{28}\text{Si}, 4n)$ reaction. The 12^+ 2628 keV isomer with a half-life $T_{1/2} = 350 \text{ ns}$ [1] was well excited (see the delayed spectrum of Fig. 1). The modulation pattern obtained from the sum of the time spectra for the 174, 280, 421, and 575 keV transitions present in the decay of this isomer is illustrated in Fig. 5. The theoretical curve was calculated by applying a multilevel formalism [28] taking into account the presence of short-lived isomers in the decay of the 12^+ isomer [1]. Note that in this case, the

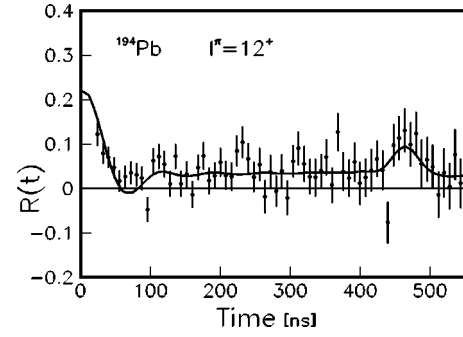


FIG. 5. Quadrupole interaction pattern for the 12^+ isomer in ^{194}Pb in solid Hg at a temperature of 170 K and the least-squares fit.

longer lifetime allowed us to see the peak at $T_0/4$, which gives strong support for the use of a single quadrupole interaction frequency in the data analysis. A value of 203(10) MHz was derived for the quadrupole coupling constant, leading to the quadrupole moment $|Q(12^+)| = 0.48(3) \text{ eb}$, in excellent agreement with the previously reported value of $0.49(3) \text{ eb}$ [17], obtained in a TDPAD measurement in which a solid Hg host was also used, but at a higher temperature of 216 K. It is worthwhile to mention that a frozen Hg target could recrystallize not necessarily as polycrystal, but as single crystal of unknown orientation [15]. This would seriously affect the analysis. The observed quadrupole interaction pattern for the 12^+ state in ^{194}Pb and the obtained quadrupole moment in good agreement with a previous result, has proved that this did not happen, and that our target preparation technique favored the Hg solidification as polycrystal.

IV. DISCUSSION

The g factors and spectroscopic quadrupole moments determined in the present work for the $21/2^-$ and $33/2^+$ isomers are compared in Table I with theoretical estimates. In Table I are also included the static moments reported in Ref. [14] for the $13/2^+$ low-lying state in ^{193}Pb .

The negative small values of the g factor for the $33/2^+$ and $21/2^-$ states are indicative for dominant neutron quasi-particle configurations. They were compared with the empirical g factors, g_{emp} , calculated using the additivity formulas and the following experimental values for the g factors of the coupling states: $g(12^+, ^{192,194}\text{Pb}) = -0.173(2)$, $g(3/2^-, ^{197}\text{Pb}) = -0.716(1)$, and $g(5/2^-, ^{201}\text{Pb}) = +0.270(1)$ [1]. The g factors of the $13/2^+$ and $33/2^+$ states coincide within errors (see Table I), which gives support to the description of the $33/2^+$ state by the $(1i_{13/2})^3$ three-neutron configuration. The g factors of the $(1i_{13/2})^n$ states in the lead nuclei exhibit a gradual decrease when going towards more neutron deficient isotopes, from $g = -0.154(1)$ in ^{200}Pb to $g = -0.180(1)$ in ^{191}Pb [1]. The presently derived g factor for the $33/2^+$ state in ^{193}Pb fits well into this systematics. The dependence of the g factors on the neutron number has been discussed by Stenzel *et al.* [17,26], and has been attributed to the reduction of the $M1$ core polarization due to the blocking of $i_{13/2} - i_{11/2}$ spin flip excitations with decreasing occupation of the $1i_{13/2}$ shell.

TABLE I. Experimental electromagnetic moments for neutron isomeric states in ^{193}Pb compared with theoretical estimates (see the text for details).

I^π	Configuration	g_{exp}	g_{emp}	g_{PBCS}	g_{PQTAC}	$ Q_{\text{exp}} (\text{eb})$	$Q_{\text{PBCS}}(\text{eb})$	$Q_{\text{PQTAC}}(\text{eb})$
$13/2^+$	$\nu 1i_{13/2}$	$-0.177(1)^a$		-0.149	-0.172	$+0.195(10)^a$	+0.20	+0.25
$33/2^+$	$\nu(1i_{13/2})^3$	0.171(9)	-0.177(1)	-0.147	-0.174	0.45(4)	+0.45	+0.46
$21/2^-$	$\nu(1i_{13/2})^2_{12^+} \otimes 3p_{3/2}$	-0.059(11)	-0.102(2)	-0.091	-0.108	0.22(2)	+0.24	+0.26
	$\nu(1i_{13/2})^2_{8^+} \otimes 2f_{5/2}$		-0.068(2)					

^aTaken from Ref.[14].

The $21/2^-$ state could arise by coupling two neutrons in the $1i_{13/2}$ orbital with one neutron in an available negative parity orbital. As seen in Table I, the experimental g factor is close to the empirical g factor values estimated for the $(1i_{13/2})^2_{8^+} \otimes 2f_{5/2}$ and $(1i_{13/2})^2_{12^+} \otimes 3p_{3/2}$ configurations. We note that a similar value, $g = -0.0506(6)$, has been reported previously for the g factor of the $21/2^-$ 1.15 μs isomeric state in ^{197}Pb , and the same configurations were considered [17]. More insight into the structure of the investigated states has been obtained by comparing their electromagnetic moments with the theoretical predictions of two different models, namely, the number-projected BCS (PBCS) and the pairing plus quadrupole tilted-axis cranking (PQTAC) models.

A. PBCS calculations

A microscopic description of odd-mass $^{193-205}\text{Pb}$ nuclei has been recently done within a standard BCS approximation in a number-projected one- and three-quasiparticle neutron space in which the projection was performed after the minimization of the ground state energy [8]. A surface delta interaction was used for the residual nucleon-nucleon interaction. In this approach, a pure $(1i_{13/2})^3$ configuration was assigned to the $33/2^+$ state in all investigated lead nuclei, while for the $21/2^-$ state a change of configuration along the isotopic chain was predicted. The wave function of this state was calculated to be dominated by the coupling of two neutrons in the $1i_{13/2}$ orbital with the $3p_{1/2}$ orbital in ^{205}Pb and with the $2f_{5/2}$ orbital in $^{201,203}\text{Pb}$, while in $^{193,195,197}\text{Pb}$ the coupling with the $3p_{3/2}$ orbital has the largest contribution. The g factors of the neutron states in ^{193}Pb , derived in the PBCS approach with an effective gyromagnetic ratio $g_s^{\text{eff}} = 0.5 g_s^{\text{free}}$ [8] are shown in Table I. The calculated g_{PBCS} values are in satisfactory agreement with the measured g factors.

In the PBCS calculations reported in Ref. [8] effective neutron charges of $e_\nu^{\text{eff}} = 0.5 e$ and $e_\nu^{\text{eff}} = 1.0 e$ were used to evaluate the electric quadrupole moments. The core polarization charges for single particle orbits around doubly magic ^{208}Pb were calculated microscopically by Sagawa and Arima [29]. On the basis of these calculations and the comparison with measured quadrupole moments for neutron single particle states, an effective neutron charge close to $1.0 e$ has been suggested [29,30]. The quadrupole moments of the $13/2^+$, $33/2^+$, and $21/2^-$ states in $^{193-205}\text{Pb}$, calculated with the PBCS approach and $e_\nu^{\text{eff}} = 1.0 e$ [8], are compared in Fig. 6 with the known experimental moments from Ref. [1] and

the present work. In the case of the $13/2^+$ and $33/2^+$ states a smooth dependence of the quadrupole moments with the neutron number is predicted by the PBCS approach that takes explicitly into account the occupation number of the neutron $1i_{13/2}$ orbital. However, while the quadrupole moment of the $13/2^+$ state in ^{205}Pb agrees with the value calculated using $e_\nu^{\text{eff}} = 1.0 e$, the values calculated in the neutron deficient nuclei are too small compared to the experimental data. In order to reproduce the measured moments for the

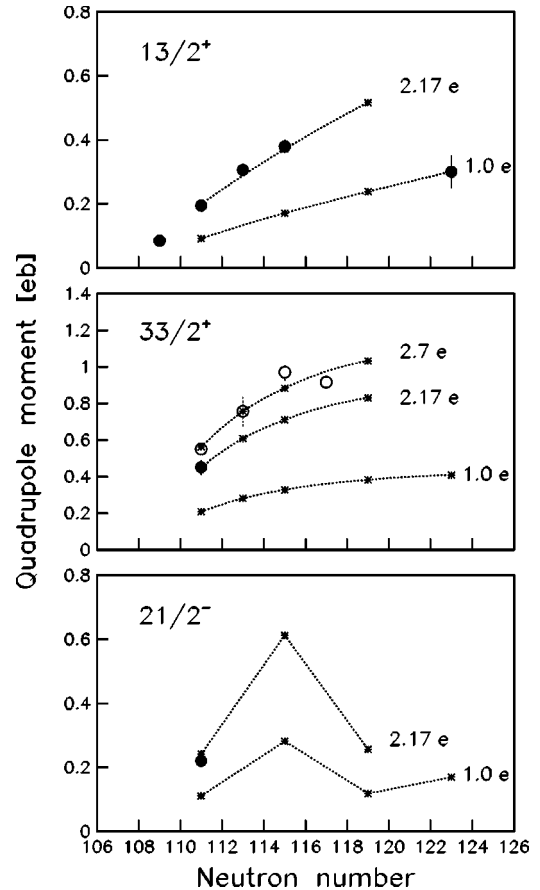


FIG. 6. Experimental spectroscopic quadrupole moments in light lead nuclei for the $13/2^+$, $33/2^+$, and $21/2^-$ states (from Ref. [1] and the present work) obtained in static moment measurements (full circle) and derived from $B(E2)$ data (open circle) compared with calculated values (small star symbol) within the PBCS approach [8] and various values for the effective neutron charge e_ν^{eff} . The theoretical values are connected by dotted lines in order to guide the eye.

$13/2^+$ states in ^{193}Pb and ^{197}Pb within the PBCS approach, the effective neutron charge has to be scaled to $e_\nu^{\text{eff}}=2.17 e$. We note that this scaling is, however, strongly dependent on the correctness of the occupation of the neutron $1i_{13/2}$ orbital. There might be a correlation between occupation and effective charge in the isotopic evolution. Using the increased effective charge $e_\nu^{\text{eff}}=2.17 e$ the calculated quadrupole moments Q_{PBCS} for the $33/2^+$ and $21/2^-$ states in ^{193}Pb are in very good agreement with the measured moments reported in the present work (see Table I and Fig. 6). The calculated quadrupole moments for the $21/2^-$ state show an irregular dependence on the neutron number (see the lower panel of Fig. 6), reflecting the change of the dominant configuration as discussed above. The good accordance of the measured quadrupole moment in ^{193}Pb with the calculated one, gives support to the $(1i_{13/2})_{12^+}^2 \otimes 3p_{3/2}$ configuration assignment.

The need to use an increased effective neutron charge in order to describe the quadrupole moments of the neutron states in light lead nuclei reflects the increased $E2$ polarization effect of valence neutrons when going further from the $N=126$ closed shell. We note that a similar increased $E2$ polarization charge was reported previously [16,17] in an analysis of the quadrupole moments of the 12^+ two-quasineutron states in $^{194-200}\text{Pb}$ within a two-quasiparticle Tamm-Dancoff approach. This finding indicates that the core polarization is rather stable and independent of the involved configuration.

The $33/2^+$ state appears systematically as an isomer in the odd-mass $^{193-199}\text{Pb}$ and deexcites by an $E2$ transition to the $29/2^+$ state [1]. While the static quadrupole moment provides information on the diagonal terms of the $E2$ matrix, the transition probability gives information on nondiagonal terms. Unfortunately, in the PBCS study of Ref. [8] no transition probability was reported. Assuming pure $(1i_{13/2})^3$ configurations for the $33/2^+$ and $29/2^+$ states and applying the shell model equations for the three-particle system and angular momentum recoupling techniques [31], the $B(E2)$ reduced transition probability may be related to the quadrupole moment of the $33/2^+$ state by the expression:

$$|eQ[(1i_{13/2})^3, 33/2^+]| = 7.68[B(E2; 33/2^+ \rightarrow 29/2^+)]^{1/2}.$$

The $B(E2)$ values were evaluated with the lifetimes of the $33/2^+$ states taken from the present work for ^{193}Pb and from Ref. [1] for $^{195-199}\text{Pb}$. The internal conversion coefficients calculated in Ref. [32] were used. The quadrupole moments deduced from the $B(E2)$ data are shown in the middle panel of Fig. 6 together with the value obtained in the present TDPAD measurement for the $33/2^+$ state in ^{193}Pb . As seen in the Fig. 6, the quadrupole moment derived in ^{193}Pb from $B(E2)$ is larger than the value obtained in the static quadrupole moment measurement. An even higher effective charge, of about $2.7 e$, is necessary in order to reproduce the moments derived from lifetime data within the PBCS approach. We note that the relation between the quadrupole moment and the reduced transition probability, given above, is strictly valid only when the seniority is a good quantum number. The large effective charges needed clearly point to large core excitation contributions including protons, too, i.e., more com-

plicated wave functions. So it is not surprising at all that inferred and measured spectroscopic quadrupole moments show a different isotopic evolution.

The enhancement of the core polarization for neutron states in light lead nuclei, revealed in the previous [16,17] and present quadrupole moment studies, shows a saturation for neutron number $N < 118$. A similar effect has been evidenced for proton states in translead ($Z > 82$) neutron deficient nuclei [30]. It has been shown that the increase in the quadrupole moments of the 8^+ proton isomers in Po nuclei with decreasing neutron number can be described by a particle-vibrational core model [33]. However, one has to note that in the case of proton states the quadrupole moments are negative and associated with weakly deformed oblate shapes, while the positive quadrupole moments of the neutron states indicate small prolate shapes.

B. PQTAC calculations

The tilted axis cranking model based on the pairing plus quadrupole interaction [13,34] has been extensively used in the light lead nuclei to describe the observed magnetic rotational bands. In the present study we applied this model to calculate the static moments of neutron isomers. The calculations were essentially done within the pairing plus quadrupole model, as for the considered states the tilt angle is zero and there is no rotation. For the neutron pairing the experimental odd-even mass difference Δ_{oe} has been used for the $13/2^+$ states. In the case of the two- and three-quasineutron states the pairing was taken as $0.75 \Delta_{\text{oe}}$. In deriving the g factors an effective gyromagnetic ratio $g_s^{\text{eff}}=0.6 g_s^{\text{free}}$ was used. The quadrupole-quadrupole coupling constant, which controls the size of the deformation, has been adjusted in order to reproduce the experimental quadrupole moment of the $\nu(1i_{13/2})^2 12^+$ isomer in ^{194}Pb . For the other isotopes this value was scaled with $A^{-5/3} r_{\text{osc}}^{-4}$, where r_{osc} is the oscillator length [34].

The calculated g factors, g_{PQTAC} , and spectroscopic quadrupole moments, Q_{PQTAC} , for the neutron states in ^{193}Pb are included in Table I. They are in good agreement with the experimental values. Small prolate deformations $\epsilon_2 = 0.013, 0.015$, and 0.026 , have been calculated with PQTAC for the $13/2^+$, $21/2^-$, and $33/2^+$ states, respectively.

The quadrupole moments calculated within the PQTAC model, as well as the measured values for the neutron states involving the $\nu(1i_{13/2})^n$ configuration in odd- and even-mass lead isotopes, are illustrated in Fig. 7. In the case of the 12^+ isomeric states, the quadrupole moments obtained from both static moment and transition probability measurements are shown. To deduce the quadrupole moment from $B(E2)$ the relation [16]:

$$|eQ[(1i_{13/2})^2, 12^+]| = 10.38 [B(E2; 12^+ \rightarrow 10^+)]^{1/2},$$

has been used. The $B(E2)$ values were calculated using transition energies and lifetimes from Ref. [35] for $^{190,192}\text{Pb}$ and from Ref. [1] for the heavier isotopes. One notes from Fig. 7 that with decreasing neutron number the quadrupole moments derived from transition probabilities are becoming larger than the values obtained in static moment measure-

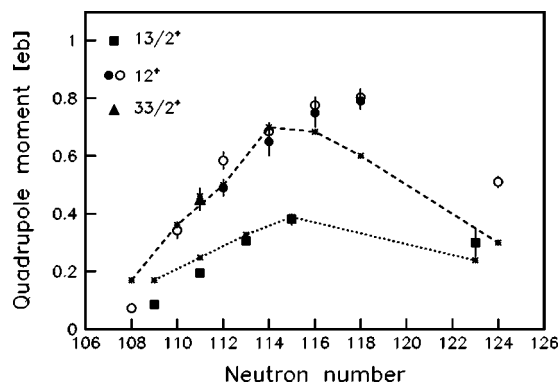


FIG. 7. Experimental spectroscopic quadrupole moments in light lead nuclei for the $13/2^+$, 12^+ , and $33/2^+$ states (from Ref. [1] and the present work) compared to pairing plus quadrupole tilted-axis cranking calculations (small star symbol). For the 12^+ states quadrupole moments obtained in static moment measurements (full symbol) and derived from $B(E2)$ (open symbol) are shown. The theoretical values are connected by lines (dotted for the $13/2^+$ state, dashed for the 12^+ state) in order to guide the eye.

ments. This feature is similar to that observed in the case of the $\nu(1i_{13/2})^3$ $33/2^+$ isomer in ^{193}Pb , as discussed above. An overall good description of the experimental quadrupole moments of the neutron states is obtained within the pairing plus quadrupole model (see Fig. 7). The observed evolution of the quadrupole moments of the $13/2^+$ and 12^+ along the isotopic chain is rather well reproduced by the calculations. The decrease of the quadrupole moments with decreasing N is caused by the shift of the neutron chemical potential toward the middle of the $1i_{13/2}$ neutron shell, where the quadrupole moment of the quasiparticle is zero. It reflects the gradual change of the quasineutron from a hole-type excitation (positive quadrupole moment) to a particle-type excitation (negative quadrupole moment). In contrast to the PBCS calculations, which assume a spherical shape, PQTAC describes the quadrupole moments well without resorting to effective charges. This indicates that the quadrupole polarization of the core is properly accounted for, which is an important finding, because the correct description of the magnetic rotational bands by means of the TAC model relies on it.

V. CONCLUSIONS

In this work we have investigated the g factors and the spectroscopic quadrupole moments for two high-spin iso-

meric states, $21/2^-$ and $33/2^+$, in ^{193}Pb . The results allowed us to assign three-neutron configurations to the investigated states. For the first time, quadrupole moments for three-quasineutron states in the neutron deficient lead isotopes were reported. The measured nuclear moments were analyzed within a microscopic BCS approach in a number-projected one- and three-quasiparticle neutron space, and in the pairing plus quadrupole tilted-axis cranking approach. Both models describe quite well the measured g factors with reasonable effective g_s factors. The PBCS calculations with an effective neutron charge of $e_\nu^{\text{eff}}=1.0 e$, which reproduce the quadrupole moments of neutron states in nuclei near the $N=126$ closed shell, are underestimating the quadrupole moments in the light lead nuclei. A much larger effective neutron charge of $e_\nu^{\text{eff}}=2.17 e$ has to be used in order to reproduce the experimental data, which reflects the increased $E2$ polarization effect of valence neutrons when going further from the $N=126$ closed shell. A better description of the core polarization effects has been obtained within the PQTAC approach. Calculations performed with this model provide an overall good description of the experimental quadrupole moments of the $13/2^+$ and 12^+ quasineutron states in the lead isotopes. The quadrupole moments of the $21/2^-$ and $33/2^+$ in ^{193}Pb are nicely reproduced with the PQTAC model which predict very small prolate deformations for these three-quasineutron states. The present results show that the quadrupole polarization of the core is properly accounted for within the PQTAC model, which is an important observation, as the correct description of the magnetic rotational bands by means of this model relies on this.

ACKNOWLEDGMENTS

The authors thank the staff of the XTU-Tandem of Laboratori Nazionali di Legnaro for the high quality of the delivered pulsed beam. They are indebted to Professor Kris Heyde for interesting comments and suggestions. Support through the EU TMR Programme under Contract No. HPRI-CT-1999-00083 is acknowledged. K.V. is financially supported by FWO-Vlaanderen, Belgium. The Leuven and Bucharest groups acknowledge support from the Bilateral Fund, Contract No. BIL02/24. The Bonn group has been supported by BMBF under Contract No. 06 BN 907, and the Bucharest group by the CERES Programme of the Romanian Ministry of Education and Research, Contract No. 81/2001. D.L.B. and M.I.-B. acknowledge a NATO CLG No. 978799. D.L.B. acknowledges partial support from the Bulgarian National Science Fund under Contract No. PH-908.

- [1] *Table of Isotopes*, 8th ed., edited by R. B. Firestone and V. S. Shirley (Wiley, New York, 1996).
- [2] R. Julin, K. Helariutta, and M. Muikku, *J. Phys. G* **27**, R109 (2001).
- [3] K. Van de Vel, A. N. Andreyev, M. Huyse, P. van Duppen, J. F. C. Cocks, O. Dorvaux, P. T. Greenless, K. Helariutta, P. Jones,

- R. Julin, S. Juutinen, H. Kettunen, P. Kuusiniemi, M. Leino, M. Muikku, P. Nieminen, K. Eskola, and R. Wyss, *Phys. Rev. C* **65**, 064301 (2002), and references therein.
- [4] G. D. Dracoulis, G. J. Lane, A. P. Byrne, A. M. Baxter, T. Kibédi, A. O Macchiavelli, P. Fallon, and R. M. Clark, *Phys. Rev. C* **67**, 051301(R) (2003), and references therein.

- [5] C. G. Lindén, I. Bergström, J. Blomqvist, and C. Roulet, *Z. Phys. A* **284**, 141 (1978).
- [6] H. Helppi, S. K. Saha, P. J. Daly, S. R. Faber, T. L. Khoo, and F. M. Bernthal, *Phys. Rev. C* **23**, 1446 (1981).
- [7] N. Sandulescu, A. Insolia, B. Fant, J. Blomqvist, and R. J. Liotta, *Phys. Lett. B* **288**, 235 (1992).
- [8] C. A.P. Ceneviva, L. Losano, N. Teruya, and H. Dias, *Nucl. Phys. A* **619**, 129 (1997), and references therein.
- [9] K. Heyde, J. Jolie, J. Moreau, J. Ryckbusch, M. Waroquier, P. Van Duppen, M. Huyse, and J. L. Wood, *Nucl. Phys. A* **466**, 189 (1987).
- [10] G. Baldsiefen, H. Hübel, W. Korten, D. Mehta, N. Nenoff, B. V. Thirumala Rao, P. Willsau, H. Grawe, J. Heese, H. Kluge, K. H. Maier, R. Schubart, S. Frauendorf, and H. J. Maier, *Nucl. Phys. A* **574**, 521 (1994).
- [11] Amita, A. K. Jain, and B. Singh, *At. Data Nucl. Data Tables* **74**, 283 (2000).
- [12] S. Frauendorf, *Z. Phys. A: Hadrons Nucl.* **358**, 163 (1997).
- [13] S. Frauendorf, *Nucl. Phys. A* **557**, 259c (1993).
- [14] S. B. Dutta, R. Kirchner, O. Klepper, T. U. Kühl, D. Marx, G. D. Sprouse, R. Menges, U. Dinger, G. Huber, and S. Schröder, *Z. Phys. A: Hadrons Nucl.* **341**, 39 (1991).
- [15] H.-E. Mahnke, T. K. Alexander, H. R. Andrews, O. Häusser, P. Taras, D. Ward, E. Dafni, and G. D. Sprouse, *Phys. Lett.* **88B**, 48 (1979).
- [16] S. Zywietz, H. Grawe, H. Haas, and M. Menningen, *Hyperfine Interact.* **9**, 109 (1981).
- [17] C. Stenzel, H. Grawe, H. Haas, H.-E. Mahnke, and K. H. Maier, *Z. Phys. A* **322**, 83 (1985).
- [18] K. Vyvey, S. Chmel, G. Neyens, H. Hübel, D. L. Balabanski, D. Borremans, N. Coulier, R. Coussement, G. Georgiev, N. Nenoff, S. Pancholi, D. Rossbach, R. Schwengner, S. Teughels, and S. Frauendorf, *Phys. Rev. Lett.* **88**, 102502 (2002).
- [19] K. Vyvey, D. Borremans, N. Coulier, R. Coussement, G. Georgiev, S. Teughels, G. Neyens, H. Hübel, and D. L. Balabanski, *Phys. Rev. C* **65**, 024320 (2002).
- [20] J. M. Lagrange, M. Pautrat, J. S. Dionisio, Ch. Vieu, and J. Vanhorenbeeck, *Nucl. Phys. A* **530**, 437 (1991).
- [21] G. Baldsiefen, M. A. Stoyer, J. A. Cizewski, D. P. McNabb, W. Younes, J. A. Becker, L. A. Bernstein, M. J. Brinkman, L. P. Farris, E. A. Hebry, J. R. Hughes, A. Kuhnert, T. F. Wang, B. Cederwall, R. M. Clark, M. A. Delwplanque, R. M. Diamond, P. Fallon, I. Y. Lee, A. O. Macchiavelli, J. Oliveira, F. S. Stephens, J. Burde, D. T. Vo, and S. Frauendorf, *Phys. Rev. C* **54**, 1106 (1996).
- [22] L. Ducroux, A. Astier, R. Duffait, Y. Le Coz, M. Meyer, S. Perries, N. Redon, J. F. Sharpey-Schafer, A. N. Wilson, R. Lucas, V. Méot, R. Collatz, I. Deloncle, F. Hannachi, A. Lopez-Martens, M. G. Porquet, C. Schück, F. Azaiez, S. Bouneau, C. Bourgeois, A. Korichi, N. Poffé, H. Sergolle, B. J. P. Gall, I. Hibbert, and R. Wadsworth, *Z. Phys. A* **356**, 241 (1996).
- [23] S. Chmel, F. Brandolini, R. V. Ribas, G. Baldsiefen, A. Görden, M. De Poli, P. Pavan, and H. Hübel, *Phys. Rev. Lett.* **79**, 2002 (1997).
- [24] D. L. Balabanski, M. Ionescu-Bujor, A. Iordachescu, D. Bazzacco, F. Brandolini, D. Bucurescu, S. Chmel, M. Danchev, M. De Poli, G. Georgiev, H. Haas, H. Hübel, N. Marginean, R. Menegazzo, G. Neyens, P. Pavan, G. Rainovski, C. Rossi Alvarez, C. A. Ur, K. Vyvey, and S. Frauendorf, *Phys. Rev. Lett.* (to be published).
- [25] D. L. Balabanski, M. Ionescu-Bujor, A. Iordachescu, D. Bazzacco, F. Brandolini, D. Bucurescu, S. Chmel, M. Danchev, M. De Poli, G. Georgiev, H. Haas, H. Hübel, N. Marginean, R. Menegazzo, G. Neyens, P. Pavan, G. Rainovski, C. Rossi Alvarez, C. A. Ur, K. Vyvey, and S. Frauendorf, *Eur. Phys. J. A* **20**, 191 (2004).
- [26] C. Stenzel, H. Grawe, H. Haas, H.-E. Mahnke, and K. H. Maier, *Nucl. Phys. A* **411**, 248 (1983).
- [27] E. Dafni, R. Bienstock, M. H. Rafailovich, and G. D. Sprouse, *At. Data Nucl. Data Tables* **23**, 315 (1979).
- [28] E. Dafni, M. H. Rafailovich, T. Marshall, G. Schatz, and G. D. Sprouse, *Nucl. Phys. A* **394**, 245 (1983).
- [29] H. Sagawa and A. Arima, *Phys. Lett. B* **202**, 15 (1988).
- [30] G. Neyens, *Rep. Prog. Phys.* **60**, 633 (2003).
- [31] K. L. G. Heyde, *The Nuclear Shell Model* (Springer, Berlin, 1994).
- [32] R. S. Hager and E. C. Seltzer, *Internal conversion table*, <http://www.nndc.bnl.gov/nndc/physco>
- [33] G. Neyens, S. Ternier, K. Vyvey, N. Coulier, R. Coussement, and D. L. Balabanski, *Nucl. Phys. A* **625**, 668 (1997).
- [34] S. Frauendorf, *Nucl. Phys. A* **677**, 115 (2000).
- [35] G. D. Dracoulis, T. Kibédi, A. P. Byrne, A. M. Baxter, S. M. Mullins, and R. A. Bark, *Phys. Rev. C* **63**, 061302(R) (2001).